Spin-dependent studies of the dynamics of He^+ ion neutralization at a Au(100) surface

D. L. Bixler, J. C. Lancaster, F. J. Kontur, P. Nordlander, G. K. Walters, and F. B. Dunning
Department of Physics and the Rice Quantum Institute, Rice University, P.O. Box 1892, Houston, Texas 77251-1892
(Received 21 December 1998)

Spin labeling techniques, specifically the use of electron-spin-polarized He^+ ions coupled with energy-resolved measurements of the ejected electron polarization, are used to study the dynamics of He^+ neutralization at a Au(100) surface. A marked correlation in the spins of the electrons involved in the Auger neutralization process is observed that is particularly pronounced at the highest ejected electron energies. A theoretical model is presented that explains the general characteristics of the data by considering the perturbation in the surface electronic structure induced by the presence of the (polarized) He^+ ion. This model, which includes the effects of ion velocity parallel to the surface, shows that the induced density of states is spin dependent, the spin dependence being most pronounced in the vicinity of the Fermi energy. [S0163-1829(99)13335-6]

INTRODUCTION

The dynamics of ion neutralization at surfaces have been investigated both by analyzing the energy distributions of electrons ejected from the surface[1] and by measuring the number, and charge state distribution, of particles produced through reflection of incident ions.[2] Here, we demonstrate a powerful method for probing such dynamics that makes use of spin labeling techniques, specifically the use of incident electron-spin-polarized He^+ ions coupled with energy-resolved measurements of the ejected electron polarization. This approach complements the earlier investigations and provides insights into the perturbations in local surface electronic structure induced by the presence of the ion.

Conventional models[1] suggest that at clean high-work function metal surfaces He^+ ions undergo Auger neutralization (AN) in which an electron from the metal tunnels into the He^+1s core hole. The energy liberated is communicated to a second electron in the metal, which, if the energy transfer is sufficient, can be ejected from the surface. This AN process results in a relatively structureless ejected electron-energy distribution that reflects, approximately, a self-convolution of the local density of electronic states at the surface. However, earlier studies using spin-polarized $He(2^3S)$ metastable atoms,[3,4] which undergo resonance ionization as they approach a high-work function metal surface, have suggested that the presence of a (polarized) He^+ ion can lead to a strong spin-dependent local perturbation in the surface electronic structure. In particular, the data suggest that the ion can, in essence, locally ''magnetize'' the surface. In the present paper, we have examined this behavior directly using a beam of polarized He^+ ions incident on a clean Au(100) surface. A marked correlation in the spins of the electrons involved in the Auger neutralization process is observed that is particularly pronounced at the highest ejected electron energies. A theoretical model is presented that explains the general characteristics of the data by considering the perturbation in the surface electronic structure that results from the presence of the polarized He^+ ion. The major perturbations to the surface electronic structure are associated with interactions that involve the helium $2s$ orbital. Near the surface, the 2^1S and 2^3S atomic levels each shift upward but broaden to such an extent that they extend below the Fermi level ε_F allowing each to be partially filled by electrons from the metal. This increases the local density of states in the vicinity of ε_F and, because the 2^1S level lies significantly higher in energy than the 2^3S level, this increase is spin dependent resulting in a marked spin dependence in the induced local density of states. The calculations include the effects of ion velocity parallel to the surface which, it is shown, can influence the polarization of the ejected electrons.

EXPERIMENTAL METHOD

The present apparatus[5] is shown schematically in Fig. 1. Polarized He^+ ions extracted from an optically pumped rf-excited helium discharge are formed into a beam by a series of electrostatic lenses and directed onto the Au(100) target surface. The energy distribution of the ejected electrons is measured using a retarding potential-energy analyzer; their polarization is determined using a compact Mott polarimeter.

The central component of the ion source is a weak, rf-excited helium discharge that is contained in a cylindrical Pyrex cell. In such discharges, Penning ionization reactions of the type

$$He(2^{1,3}S) + He(2^{1,3}S) \rightarrow He^+ + He(1^1S) + e^- \qquad (1)$$

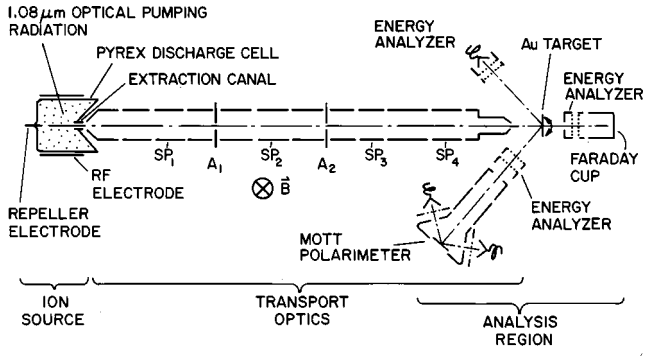

FIG. 1. Schematic diagram of the apparatus. The lens elements labeled $SP_1 \ldots SP_4$ also serve as steering plates. A_1 and A_2 are small beam defining apertures.

involving He($2^{1,3}S$) metastable atoms present in the discharge contribute significantly to the overall ion production.[6] If the He(2^3S) atoms are spin polarized by optical pumping, spin angular momentum conservation leads to the formation of polarized He^+ ions. Because the performance of the source is degraded by the presence of impurities in the discharge, helium gas is flowed through the cell. The cleanness of the discharge is monitored using a low-resolution spectroscope; if no spectral lines other than those of helium are detected, the source will typically perform well.

A weak-magnetic field of ~2 G is applied across the discharge cell (and the entire ion beam line) to establish and maintain a well defined quantization axis. The 2^3S atoms in the discharge are polarized by optical pumping using circularly polarized 1.083 μm $2^3S \rightarrow 2^3P$ radiation. This is provided by a system comprised of a distributed Bragg reflector (DBR) laser diode coupled to a Yb-doped fiber amplifier,[7] which yields output powers $\gtrsim$ 0.5 W. Use of right-hand (left-hand) circularly polarized radiation preferentially transfers, or pumps, 2^3S atoms into the $m_J = +1(-1)$ magnetic sublevel. The relative densities n_+, n_0 and n_- of 2^3S atoms in the $m_J(m_S) = +1$, 0, and -1 sublevels, respectively, are obtained, as described previously,[8] by measuring the absorption of a weak circularly polarized 1.083-μm probe beam that is provided by a second DBR laser diode. The output frequency of this laser is scanned by varying the drive current to allow separate absorption measurements at the $2^3S_1 \rightarrow 2^3P_0(D_0)$, $2^3S_1 \rightarrow 2^3P_1(D_1)$, and $2^3S_1 \rightarrow 2^3P_2(D_2)$ transitions. Such measurements show that, when pumping on the $2^3S_1 - 2^3P_1(D_1)$ transition, the present laser system can provide He(2^3S) polarizations in the discharge, defined by

$$P_z = \langle S_z \rangle = \frac{(n_+ - n_-)}{n_+ + n_0 + n_-}, \tag{2}$$

of typically 0.65 to 0.75. The metastable atom (and thus ion beam) polarization can be easily reversed by changing the sense of circular polarization of the optical pumping radiation.

Ions formed in the discharge are extracted through a short canal with the aid of a small bias applied to a repeller electrode. The emergent ions are formed into a beam and transported to the target surface by a system of electrostatic lenses. The ion transport energies are relatively high (~200–250 eV) to minimize deflections due to the transverse field that defines the quantization axis. To correct these deflections, the lenses indicated were divided into four quadrants allowing them to double as beam steering elements by application of small transverse electric fields. Ions emerging from the extraction canal have a broad energy distribution, $\gtrsim$ 20 eV, that depends on the discharge pressure and intensity. The energy distribution of those ions that impact the target surface is reduced by taking advantage of the chromatic aberration in the lens system. The ion transport system was designed with two intermediate foci where small apertures, labeled A_1 and A_2 in Fig. 1, were located. [The second aperture A_2 also provides a convenient vacuum break between the intermediate and final (UHV) vacuum chambers.] Only ions within a narrow energy range, ~3–5 eV full width half maximum, are focused through both apertures. The energy distribution, and total current, of the ions incident on the target surface was measured by moving the target and allowing the beam to enter a Faraday cup equipped with a retarding potential-energy analyzer. To facilitate changing the ion impact energy at the (grounded) target, the power supplies and potential dividers used to bias the repeller electrode, extraction canal, and elements of the ion transport system up to, and including, the second aperture A_2 are all referenced to a common potential. By varying this potential, the energy of the ions relative to ground can be adjusted without changing the ion extraction conditions or the focusing of the optics through A_2. The potentials applied to the lens elements following A_2 must, however, be individually adjusted as the beam energy is changed to maintain a good focus on the target surface. Using this technique, the ion impact energy at the target can be varied from $\lesssim$ 15 to $\gtrsim$ 300 eV.

The ion beam purity was checked using time of flight techniques by pulsing the transverse voltages applied to the first set of steering plates. At the source operating pressures used in this work ($\lesssim$ 0.3 torr) only He^+ ions could be detected. The He^+ beam polarization, defined by

$$P_+ = \frac{N_+ - N_-}{N_+ + N_-}, \tag{3}$$

where N_+ and N_- are the number of ions in the $M_J(M_S) = +\frac{1}{2}$ and $-\frac{1}{2}$ magnetic sublevels, respectively, is determined by allowing the beam to strike the clean Au(100) target surface and measuring the polarization of the ejected electrons. This polarization, specified by

$$P_e = \frac{n_\uparrow - n_\downarrow}{n_\uparrow + n_\downarrow}, \tag{4}$$

where $n_\uparrow$ and $n_\downarrow$ are the number of electrons in the $m_s = +\frac{1}{2}$ and $-\frac{1}{2}$ states, respectively, was determined by directing the ejected electrons into a compact retarding-potential Mott polarimeter.[9] Earlier work in this laboratory[4] using a beam of polarized thermal-energy He(2^3S) atoms [which undergo resonance ionization as they approach a Au(100) surface] has shown the electrons involved in Auger neutralization of such ions are correlated in spin, resulting in an ejected electron polarization that is, on average, ~0.3 times the polarization of the incident ions. Using this known spin correlation, the incident ion polarization P_+ can be inferred from the measured electron polarization P_e, i.e., $P_+ \simeq P_e/0.3$. The earlier spin correlation studies[4] pertain to very low-ion impact energies, $\lesssim$1 eV. However, the present measurements show that the average ejected electron polarization is independent of incident ion energy, at least for ion energies in the range 10 to 250 eV, suggesting that the spin correlation is not strongly energy dependent. Under optimum operating conditions, the present source can provide ion beam currents of ~1–2 nA at the target surface with polarizations P_+ of ~0.17.

The Au(100) target surface is cleaned by repeated argon ion bombardment/thermal annealing cycles. Surface cleanness is monitored by Auger analysis and by ion neutralization spectroscopy, i.e., by measuring the energy distribution of electrons ejected from the surface as a result of He^+ ion neutralization. This distribution, which is measured using a simple retarding potential-energy analyzer, is very sensitive to surface contamination.[1,10] The ejected electron polariza-

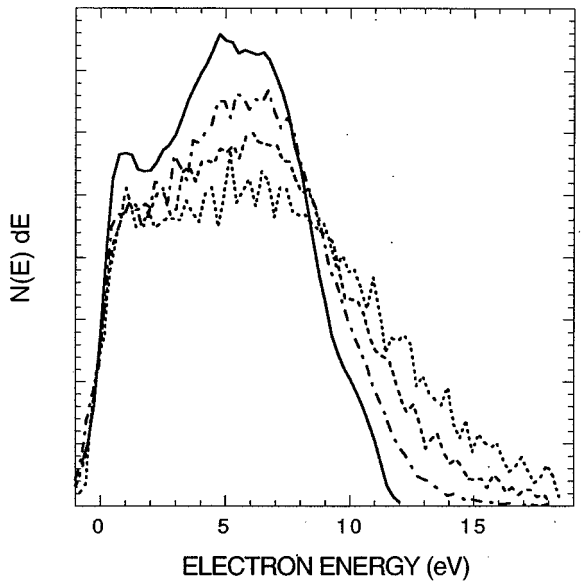

FIG. 2. Electron-energy distributions resulting from He^+ ion neutralization at a clean Au(100) surface for incident ion energies of (—.—.—.—) 16, (— — —) 60, and (---) 250 eV. (——), earlier results obtained using incident He(2^3S) metastable atoms (Ref. 4).

tions were measured using a Mott polarimeter, which was equipped with a retarding potential-energy analyzer at its input to permit energy resolved measurements. In the Mott polarimeter, the electron polarization is determined by measuring the asymmetry that results due to the spin-orbit effect when they scatter quasielastically at large angles ($\pm \sim 120°$) from a thorium target maintained at 25 kV. This asymmetry, defined as[9,11]

$$A = \frac{N_L - N_R}{N_L + N_R}, \tag{5}$$

where N_L and N_R are the numbers of electrons scattered to the left and right, respectively, is related to the component of electron spin perpendicular to the scattering plane by $P_e = A/S_{\text{eff}}$, where S_{eff} is the (known) effective scattering asymmetry. Effects associated with instrumental asymmetries are eliminated, as described elsewhere,[9,11] by undertaking measurements with the incident ion-beam polarization reversed ($P_+ \rightarrow -P_+$), which is simply accomplished by reversing the sense of circular polarization of the optical pumping radiation in the source.

RESULTS AND DISCUSSION

Ejected electron-energy distributions observed following He^+ ion neutralization at a clean Au(100) surface are presented in Fig. 2 for incident ion energies of 16, 60, and 250 eV. Also included is the energy distribution measured in earlier work that results from the deexcitation of thermal-energy He(2^3S) metastable atoms.[4] As expected, the energy distributions, which reflect a self-convolution of the local density of states, are broad and relatively featureless. The high-energy cutoff in the distributions, however, increase markedly with increasing incident ion energy. In the absence of other effects, simple arguments suggest that the maximum ejected electron energy should be given by $E_{\max} = \varepsilon_i - 2\phi$, where ε_i is the ionization energy of the ion and ϕ is the surface work function, ~5.5 eV for Au(100). The ionization energy ε_i depends on the ion-surface separation, decreasing from the value characteristic of an isolated ion ($\varepsilon_i \sim 24.6$ eV) as the surface is approached. This suggests a value $E_{\max} \lesssim 13.6$ eV, which is in reasonable accord with the value observed with He(2^3S) atoms. Several effects have been discussed that might account for the observed increase in the high-energy cutoff with increasing ion energy,[1,2,12] the two most important of which are associated with the motion of the incident ion. The first is a purely kinematic effect. In the metal, the electrons can be approximated as a semi-infinite free-electron gas. The density of states in momentum ($\vec{k}$) space for such a gas is constant. Transformation into energy space leads to a density of states $n(\varepsilon)$ that increases with increasing electron energy ε as $n(\varepsilon) \sim \varepsilon^{1/2}$. Multiplication by the Fermi-Dirac distribution function results, for relatively low temperatures, in a sharp cutoff in the density of states near the Fermi energy ε_F. In $\vec{k}$ space, this cutoff limits the occupied states to those within a sphere, termed the Fermi sphere, of radius k_F, corresponding to a Fermi velocity v_F. In the rest frame of the incident ion, the velocity distribution of electrons in the metal is shifted by an amount equal to the incident ion velocity $\vec{v}_i$. This distorts the density of electronic states as observed from the moving ion.[1,2] The effective cutoff in the density of states is increased to a new value ε_c given by $\varepsilon_c = m_e(v_F + v_i)^2/2$. For gold, $\varepsilon_F \simeq 5.5$ eV corresponding to a Fermi velocity $v_F \sim 1.4 \times 10^6\ \text{ms}^{-1}$. A He^+ ion incident at 250 eV has a velocity $v_i \sim 1.1 \times 10^5\ \text{ms}^{-1}$, resulting in a cutoff energy $\varepsilon_c \sim 6.4$ eV, i.e., in a reduction of ~1 eV in the effective surface work function. Such a decrease would lead to an increase of ~2 eV in the maximum ejected electron energy. This increase, although substantial, is somewhat less than that observed experimentally, suggesting that an additional broadening mechanism is occurring. As discussed by Hagstrum,[12] this is most likely associated with nonadiabatic excitation of electrons in the solid by the moving ion to create electron-hole pairs. Such electrons have energies above ε_F and, if they participate in the Auger neutralization process, could lead to increased ejected electron energies. Fourier analysis of the variation in the potential at a point as the ion passes by[12] suggests that the broadening due to this mechanism should increase approximately linearly with v_i and amount to ~0.5 to 1.5 eV for the present range of ion energies.

Measured ejected electron polarizations are shown in Fig. 3 as a function of the retarding potential V_R applied to the retarding grid in the energy analyzer at the input to the Mott polarimeter for ion energies of 16, 60, and 250 eV. The electron polarization is normalized to that of the incident ions. For any particular retarding potential V_R, the measured polarization represents the average polarization of all electrons ejected with energies greater than eV_R, where e is the electronic charge. A marked spin correlation is evident indicating that the electrons involved in the Auger neutralization process tend to have antiparallel spins. This can be seen, for example, by considering the specific case where the incident He^+ ions are polarized in the $M_J(M_S) = +\frac{1}{2}$, i.e., spin-up state. Because the helium ground state is a spin singlet, such

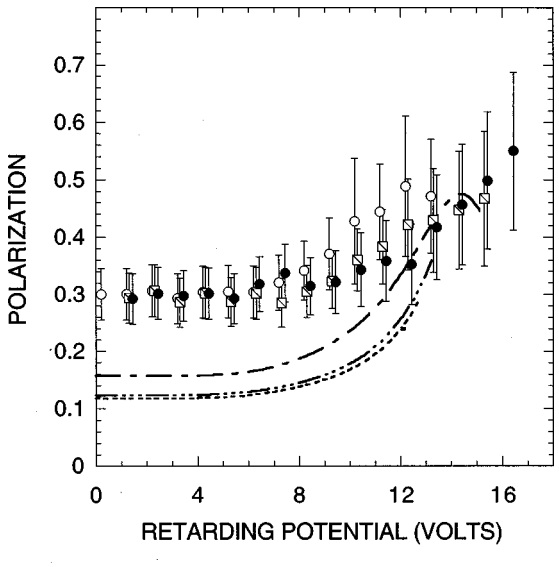

FIG. 3. Ejected electron polarizations as a function of the retarding potential V_R applied to the retarding grid in the energy analyzer at the input to the Mott polarimeter. Data points: experimental measurements for He^+ ion energies of (○) 16, (□) 60, and (●) 250 eV. Lines: theoretical predictions obtained assuming that He^+ neutralization occurs at an ion-surface separation $Z=6$ a.u. for incident He^+ ion energies of (— — —) 16, (——---) 60, and (——·——) 250 eV and assumed effective surface temperatures T_{eff} of 900, 1500, and 3000 K, respectively. The electron polarization is normalized to that of the incident ions.

ions must be neutralized by spin-down $m_s=-\frac{1}{2}$ electrons from the metal. However, as shown by experiment, this is accompanied by preferential ejection of spin-up electrons leading to the formation of singlet two-hole final states in the surface.

The general characteristics of each of the data sets in Fig. 3 are similar (and mirror the behavior observed with polarized $He(2^3S)$ atoms).[3,4] At low-to-intermediate values of retarding potential, the measured electron polarizations are essentially constant and independent of incident ion energy. However, they increase markedly at the highest retarding potentials indicating that those electrons in the high-energy tail of the electron-energy distributions have polarizations that are significantly higher than those characteristic of the rest of the distribution. This increase in polarization can be explained by considering the perturbation in surface electronic structure induced by the presence of the (polarized) He^+ ion. Calculation of such perturbations, and the energy and polarization distribution of the ejected electrons resulting from Auger neutralization, is a very challenging problem. However, a qualitative understanding of the underlying physics can be achieved by adopting some simplifying assumptions.

THEORY

A rigorous theory of the Auger neutralization of ions near a surface is still lacking. While some progress has been achieved in calculating transition matrix elements for very large atom-surface separations,[13] it is still not clear how transition-matrix elements should be calculated at typical physisorption distances. The major difficulty arises from the incomplete understanding of the influence of metallic screening on the process. (Auger transition-matrix elements depend sensitively on the dielectric function used to screen the Coulomb potential.[14]) Also, perturbations introduced by the presence of the He^+ ion near the surface could have a strong effect on the transition matrix elements.[15]

Here we neglect the energy and spin dependence of the transition-matrix elements and assume that the ejected electron currents are proportional to a simple selfconvolution of the occupied part of the surface densities of states for spin-up and spin-down electrons, $\rho_\uparrow^{\text{occ}}$ and $\rho_\downarrow^{\text{occ}}$. If, as assumed previously, the incident ions are polarized in the $M_J(M_s)=+1/2$ state, the currents of spin-up and spin-down electrons ejected from the surface with energy ω will be given by

$$I_\uparrow(\omega)\propto\int d\varepsilon'\rho_\downarrow^{\text{occ}}(\varepsilon')\rho_\uparrow^{\text{occ}}(\omega-\varepsilon_i-\varepsilon')$$
$$I_\downarrow(\omega)\propto\int d\varepsilon'\rho_\downarrow^{\text{occ}}(\varepsilon')\rho_\downarrow^{\text{occ}}(\omega-\varepsilon_i-\varepsilon'), \tag{6}$$

where ε_i is the ionization energy of the ion. When evaluating these expressions it is assumed that the He^+ ion is at a fixed atom-surface separation and is in equilibrium with the surface. In practice, the incident ion has a component of velocity perpendicular to surface. (The ions are incident at an angle $\theta\simeq 50°$ to the surface normal.) Because of this, the transition-matrix elements might also be influenced by nonadiabatic effects. However, a fully nonadiabatic treatment of the problem is presently not possible.

The presence of the (polarized) He^+ ion at the surface introduces a spin-dependent perturbation. To estimate the induced density of states, the He^+-surface interaction is treated using the Anderson Hamiltonian

$$H=\sum_{k\sigma}\varepsilon_k n_{k\sigma}+\sum_\sigma\varepsilon_\sigma n_\sigma+\frac{1}{2}\sum_{\sigma\neq\sigma'}U_{\sigma\sigma'}n_\sigma n_{\sigma'}$$
$$+\sum_{k,\sigma}V_{k\sigma}c_\sigma^+c_{k\sigma}+\sum_{k,\sigma}V_{k\sigma}^*c_{k\sigma}^+c_\sigma. \tag{7}$$

Here, ε_σ denotes the energy of the different electronic states σ of the helium atom. The subscript k refers to the Bloch momentum and band index of the metal conduction electrons. $U_{\sigma\sigma'}$ represents the intra-atomic Coulomb repulsion between the different helium states. $V_{k\sigma}$ is the hopping matrix element between the helium state $|\sigma\rangle$ and the conduction electron state in the metal $|k,\ \sigma\rangle$. It is assumed that spin is conserved during electron tunneling.

The surface is approximated using a jellium model characterized by a half-filled elliptical conduction band centered at the Fermi energy. The unperturbed density of states at the surface thus takes the form

$$\rho_\sigma^{\text{surf}}(\varepsilon-\varepsilon_F)=\frac{3}{4D}\left[1-\left(\frac{\varepsilon-\varepsilon_F}{D}\right)^2\right] \tag{8}$$

for $\varepsilon\in(-D+\varepsilon_F,\ D+\varepsilon_F)$, and $\rho_\sigma^{\text{surf}}=0$ elsewhere. For Au, we take $D=5.5$ eV, consistent with a Wigner Seitz radius of $r_s=3.01$ a.u. The major perturbation in the surface electronic structure is associated with the helium 2^3S and 2^1S atomic states. At large atom-surface separations, the 2^3S and 2^1S

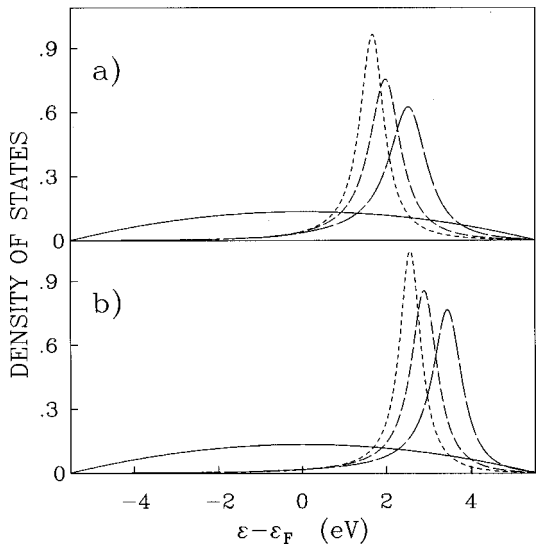

FIG. 4. Calculated induced densities of (a) spin-up and (b) spin-down states for a He^+ ion located 4 (——), 6 (− − −), and 8 (- - - -) a.u. from the surface. The solid line shows the assumed bulk density of states.

levels lie ~4.77 and 3.97 eV, respectively, below the vacuum level. The levels are relatively close to the Fermi energy of the target and therefore hybridize strongly with the surface. However, the energy separation is such that the populations in these levels will be small allowing many-electron effects to be neglected. The $U_{\sigma\sigma'}$ term in Eq. (7) can therefore be omitted enabling analytical diagonalization of the Hamiltonian.

As an atom approaches a metal surface, the energy levels shift and broaden. The distance dependence of the shift and broadening of the $He(2^3S)$ state has been calculated previously using the complex scaling method.[16] In the region outside the surface where Auger neutralization is expected to occur, i.e., at atom-surface separations Z between 4 and 8 a.u., the shift and broadening of the state can be parameterized as

$$\varepsilon_\sigma(Z)-\varepsilon_\sigma^0=\frac{27.2}{4Z}eV \tag{9}$$

and

$$\Gamma_\sigma(Z)=1.4\exp(-0.14Z)eV. \tag{10}$$

For simplicity, we assume that the shift and broadening of the $He(2^1S)$ state is the same as for the $He(2^3S)$ state.

For a He^+ ion at rest near the surface, the induced densities of spin-up and spin-down states can be calculated directly from the retarded Green's functions of the two levels, $\rho_\sigma^{\rm ind}(\varepsilon)=2\,{\rm Im}\,G_\sigma(\varepsilon)$.[17] Figure 4 shows the calculated induced density of spin-up and spin-down states for a He^+ ion located $Z=4$, 6, and 8 a.u. from the surface. The effect of the increasing shift and broadening of the atomic levels as the surface is approached is clearly apparent. For reference, Fig. 4 also includes the substrate density of states.

The effective density of surface electronic states near the He^+ ion may be written

$$\rho_\sigma^{\rm eff}(\varepsilon)=\alpha\rho_\sigma^{\rm surf}(\varepsilon)+(1-\alpha)\rho_\sigma^{\rm ind}(\varepsilon), \tag{11}$$

where α can be treated as a free parameter to be determined by fitting model predictions to the experimental data. As will be shown, reasonable fits can be obtained using $\alpha\sim0.1$. (It might be expected that α should be small since the induced states have the greatest overlap with the helium orbitals.) In equilibrium, the occupied density of states can be obtained from the total effective density of states by multiplying by a modified Fermi-Dirac distribution function.

The two effects of ion velocity discussed earlier are included in the calculations as follows. Electron-hole pair excitation is taken into account by increasing the effective surface temperature, which broadens the Fermi-Dirac distribution. As noted previously, broadening due to electron-hole pair excitation is expected to increase linearly with ion velocity. In calculating the occupied densities of states, effective surface temperatures $T_{\rm eff}$ of 300, 900, 1500, and 3000 K were used for incident ion energies of 0, 16, 60, and 250 eV, respectively. These choices of temperature lead to high-energy cutoffs in the ejected electron energy distributions that are in accord with those observed experimentally. A technique based on the Galilean transformation operator is used to model the effects of parallel velocity.[18] For an ion moving with momentum $\vec{Q}_\parallel$ parallel to the surface, the problem can be solved exactly. If matrix element effects are neglected, the finite parallel velocity can be accounted for by replacing the (broadened) Fermi-Dirac distribution function $f_{\vec{k}}$ with the quantity

$$F(\varepsilon,\vec{Q}_\parallel,T_{\rm eff})=\frac{\langle f_{\vec{k}+\vec{Q}_\parallel}\rangle_\varepsilon}{\langle f_{\vec{k}}\rangle_\varepsilon}, \tag{12}$$

where the average over $\vec{k}$ is restricted to $\varepsilon_{\vec{k}}=\varepsilon$. This averaging can be done numerically for a spherical Fermi surface.

The total occupied density of states $\rho_\sigma^{\rm occ}(\varepsilon)$ is simply obtained by multiplying $\rho_\sigma^{\rm eff}(\varepsilon)$ by $F(\varepsilon,\vec{Q}_\parallel,T_{\rm eff})$. Figure 5 shows the calculated occupied densities of spin-up and spin-down states for the ion energies employed experimentally and ion-surface separations of 4, 6, and 8 a.u. For reference, results are included for zero incident ion energy. A marked spin dependence in the density of occupied states is evident that is particularly pronounced in the vicinity of ε_F. The density of spin-up states is significantly higher than that of spin-down states. This results because, as illustrated in Fig. 4, the resonance associated with spin-up states lies ~0.8 eV lower in energy than that for spin-down states, i.e., closer to ε_F. As expected, because of kinematic effects, the density of occupied states is quite sensitive to ion energy, extending towards ever higher energies as the ion velocity is increased. Interestingly, near ε_F, the occupied density of states is not strongly dependent on the ion-surface separation Z. This results because, as can be seen from Fig. 4, although the resonances in the induced densities of states broaden as Z decreases, they also shift toward higher energies maintaining approximately the same density of states in the vicinity of ε_F. However, for energies well above ε_F a significant distance dependence is apparent.

The energy dependence of the ejected electron polarizations derived using Eqs. (6) for ion neutralization 4, 6, and 8 a.u. from the surface is shown in Fig. 6. Similar trends are evident in each data set. The calculated polarizations are sub-

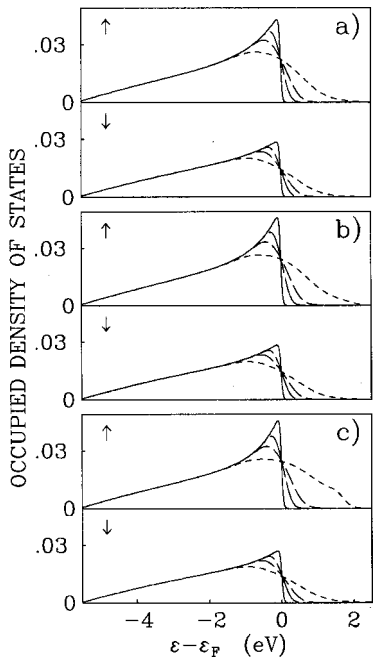

FIG. 5. Calculated occupied densities of spin-up and spin-down states for He^+ ion-surface separations of (a) 4, (b) 6, and (c) 8 a.u. The different lines are for incident ion energies of (——) 0, (—— ——) 16, (− − −) 60, and (-----) 250 eV and assumed effective surface temperatures T_{eff} of 300, 900, 1500, and 3000 K, respectively.

stantial and increase dramatically with increasing ejected electron energy, and thus with increasing incident ion energy, in qualitative agreement with the experimental results. This increase in the polarization is to be expected because, as the ejected electron energy increases, the electrons involved in the Auger neutralization process must originate from ever higher energy states where the spin dependence in the density of occupied states is most pronounced. Interestingly, theory suggests the possibility that for high-incident ion energies the polarization of the ejected electrons might reverse sign near the high-energy cutoff. This results because the calculations predict that for large ion-surface separations the occupied density of spin-down states is greater than that of spin-up states for energies $\varepsilon-\varepsilon_F \gtrsim 2$ eV. The shift of the distributions toward lower ejected electron energies with decreasing neutralization distance results from the upward shift in the ground-state energy of the ion as it approaches the surface. The low-energy cutoff in the distribution is an artifact of the simplified band structure assumed in the calculation.

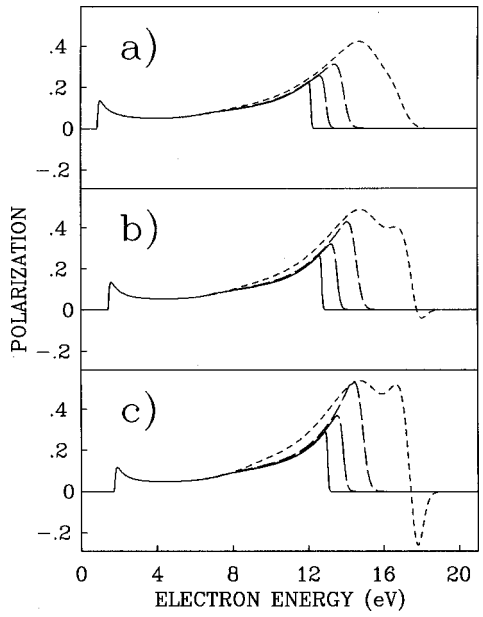

FIG. 6. Calculated energy dependence of the ejected electron polarization assuming that He^+ neutralization occurs at ion-surface separations of (a) 4, (b) 6, and (c) 8 a.u. The different lines are for incident ion energies of (——) 0, (—— ——) 16, (− − −) 60, and (-----) 250 eV and assumed effective surface temperatures of 300, 900, 1500, and 3000 K, respectively.

In order to obtain a direct comparison to experiment, where the average polarization of all electrons ejected with energies greater than some value eV_R set by the retarding potential V_R used in the energy analyzer is measured, averaged polarizations were calculated using the expression

$$P(V_R)=\frac{\int_{eV_R}^{\infty} d\omega\{I_{\uparrow}(\omega)-I_{\downarrow}(\omega)\}}{\int_{eV_R}^{\infty} d\omega\{I_{\uparrow}(\omega)+I_{\downarrow}(\omega)\}}. \tag{13}$$

Results obtained assuming that neutralization occurs at ion-surface separations Z of 4, 6, and 8 a.u. are presented in Fig. 7. The calculations are limited to retarding voltages for which the transmitted secondary electron current is at least 0.1% of the total secondary electron current. The predicted polarizations increase with increasing incident ion energy but, at least for values of $Z \lesssim 6$ a.u., this increase is small. Overall, the calculated polarizations are relatively independent of Z. The results for $Z=6$ a.u. are included in Fig. 3. Although the predicted polarizations are somewhat lower than the measured values, the general agreement between theory and experiment is quite good, especially considering the simplifying assumptions inherent in the theory. In particular, the present model correctly predicts the large increase in polarization seen at the highest retarding voltages. Although, the predicted increase depends on the widths of the spin-up and spin-down resonances in the induced density of states, i.e., on the widths and degeneracy of the helium $2^{1,3}S$ levels, the general features of the calculated spin polarizations and their dependence on ion energy are not strongly influenced by reasonable changes in the helium level parameterizations. A detailed investigation of these dependences has been presented elsewhere.[19] The resonance in the spin-down density of states lies relatively far above the Fermi level. Thus, decreasing the widths of the resonances reduces the relative contribution of spin-down states to the total density of states near ε_F. A reduction of a factor two in the widths, for example, increases the calculated maximum polarization to ~0.7. Matrix-element effects and the simple assumed shape of the conduction band might also contribute to the differences between the measured and calculated polarizations.

An additional mechanism that might contribute to the observed spin correlation has been proposed[20] that is based on the separate consideration of the transition rates associated with the ejection of spin-up and spin-down electrons. An incident (spin-up) He^+ ion must be neutralized by a spin-

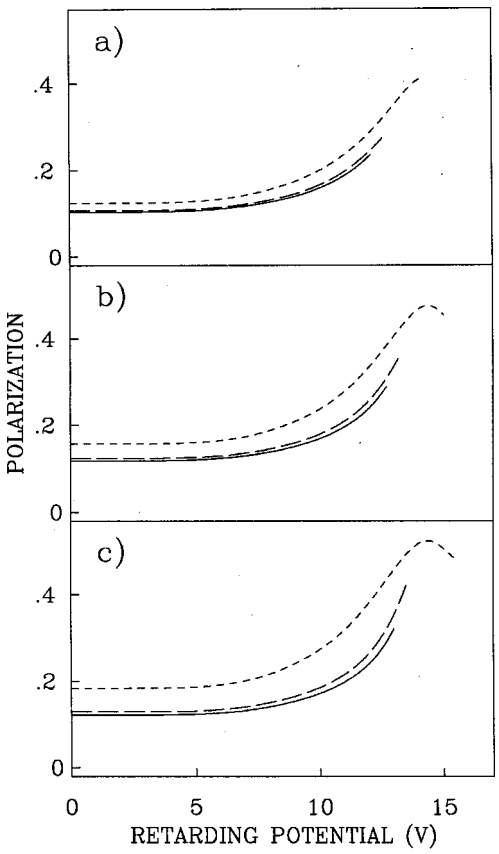

FIG. 7. Calculated ejected electron polarization as a function of the retarding potential V_R assuming that He^+ neutralization occurs at ion-surface separations Z of (a) 4, (b) 6, and (c) 8 a.u. for incident He^+ energies of (——) 16, (—— ——) 60, and (– – –) 250 eV and assumed effective surface temperatures T_{eff} of 900, 1500, and 3000 K, respectively.

down electron from the surface, but the ejected electron can have spin up or down. If Auger neutralization leads to ejection of a spin-up electron, the neutralizing and ejected electrons can be distinguished. If spin-down electron ejection occurs, it is not possible to determine for a given initial pair of spin-down electrons in the metal which is captured by the He^+ ion and which is ejected. This gives rise to two indistinguishable reaction channels and interference between these can reduce the probability for ejecting spin-down electrons as compared to that for ejecting spin-up electrons. Calculations using this model and approximate metal and atomic wave functions, and including surface screening, suggest that such interference could lead to sizable ejected electron polarizations. However, the polarization is predicted to decrease dramatically with increasing electron energy, behavior that is opposite to that observed experimentally.

CONCLUSIONS

The present paper shows that spin labeling techniques provide a powerful tool with which to investigate the dynamics of ion-surface interactions. This approach can provide insights into the perturbations in the local surface electronic structure introduced by the presence of the ion. In particular, comparisons between experimental data and the results of a simple theoretical model demonstrate that the presence of a (polarized) He^+ ion near a surface can result in a strong spin dependence in the induced density of states. Because the induced density of states results from partial filling of the broadened helium $2^{1,2}S$ levels, three basically independent mechanisms might be pictured as leading to He^+ ion neutralization: Auger neutralization, direct Auger deexcitation of the singlet state with emission of a metal electron, and indirect Auger deexcitation of the singlet or triplet states in which a metal electron fills the He $1s$ core hole with emission of the $2s$ electron. Only the latter process would lead to ejection of a polarized electron. Thus, the observed electron spin polarization might be considered as a measure of the relative importance of indirect Auger deexcitation as compared to the other processes. Further work will be required, however, to estimate the various matrix elements to better develop this picture.

ACKNOWLEDGMENTS

The experimental research was supported by the Office of Basic Energy Sciences, U.S. Department of Energy and the Robert A. Welch Foundation. The theoretical work was funded by the National Science Foundation under Grants Nos. DMR-952144 and CDA-9502791.

[1] See, for example, H. D. Hagstrum, in *Electron and Ion Spectroscopy of Solids*, edited by L. Fiermans, J. Vennik, and W. Dekeyser (Plenum, New York, 1978), p. 273; H. J. Andrä, in *Fundamental Processes of Atomic Dynamics*, edited by J. S. Briggs, H. Kleinpoppen, and H. O. Lutz (Plenum, New York, 1988), p. 631.

[2] See, for example, H. Winter, Rev. Sci. Instrum. **67**, 1674 (1996); J. Phys.: Condens. Matter **5**, A295 (1993); H. Winter, C. Auth, R. Schuch, and E. Beebe, Phys. Rev. Lett. **71**, 1939 (1993).

[3] F. B. Dunning and P. Nordlander, Nucl. Instrum. Methods Phys. Res. B **100**, 245 (1995).

[4] F. B. Dunning, D. M. Oro, P. A. Soletsky, X. Zhang, P. Nordlander, and G. K. Walters, Z. Phys. D **30**, 239 (1994).

[5] D. L. Bixler, J. C. Lancaster, R. A. Popple, F. B. Dunning, and G. K. Walters, Rev. Sci. Instrum. **69**, 2012 (1998); D. L. Bixler, J. C. Lancaster, F. J. Kontur, R. A. Popple, F. B. Dunning, and G. K. Walters, *ibid.* **70**, 240 (1999).

[6] M. V. McCusker, L. L. Hatfield, and G. K. Walters, Phys. Rev. A **5**, 177 (1972).

[7] See, for example, D. C. Hanna, R. M. Percival, I. R. Perry, R. G. Smart, P. J. Suni, and A. C. Tropper, J. Mod. Opt. **37**, 517 (1990).

[8] C. D. Wallace, D. L. Bixler, D. Huang, A. H. Wagman, F. B. Dunning, and G. K. Walters, Rev. Sci. Instrum. **67**, 1684 (1996).

[9] G. C. Burnett, T. J. Monroe, and F. B. Dunning, Rev. Sci. Instrum. **65**, 1893 (1994).

[10] D. M. Oró, P. A. Soletsky, X. Zhang, F. B. Dunning, and G. K. Walters, Phys. Rev. A **49**, 4703 (1994).

[11] F. B. Dunning, Nucl. Instrum. Methods Phys. Res. A **347**, 152 (1994).
[12] H. D. Hagstrum, Y. Takeishi, and D. D. Pretzer, Phys. Rev. **139**, A526 (1965).
[13] N. Lorente and R. Monreal, Phys. Rev. B **53**, 9622 (1996).
[14] N. Lorente and R. Monreal, Nucl. Instrum. Methods Phys. Res. B **78**, 44 (1993).
[15] N. N. Nedeljovic, R. K. Janev, and V. Y. Lazur, Phys. Rev. B **38**, 3088 (1988).
[16] F. B. Dunning, P. Nordlander, and G. K. Walters, Phys. Rev. B **44**, 3246 (1991).
[17] G. D. Mahan, *Many-Particle Physics* (Plenum, New York, 1990).
[18] J. N. M. van Wunnik, R. Brako, K. Makoshi, and D. Newns, Surf. Sci. **126**, 618 (1983).
[19] D. L. Bixler, J. C. Lancaster, F. J. Kontur, P. Nordlander, G. K. Walters, and F. B. Dunning, Nucl. Instrum. Methods Phys. Res. B (to be published).
[20] L. A. Salmi, Phys. Rev. B **46**, 4180 (1992); L. A. Salmi, R. M. C. Monreal, and S. P. Apell, Solid State Commun. **77**, 495 (1991).